Journal of Inclusion Phenomena and Molecular Recognition in Chemistry **12**: 313–332, 1992.

On the Solid-State Conformations of 18-crown-6 Complexes

THOMAS M. FYLES
Department of Chemistry, University of Victoria, Victoria, B.C. Canada V8W 3P6

and

RICHARD D. GANDOUR
Department of Chemistry, Louisiana State University, Baton Rouge, LA 70802-1804, U.S.A.

(Received: 28 September 1990; in final form: 15 December 1990)

Abstract. A procedure for displaying macrocylic torsion angles as a map on polar coordinates is discussed with reference to the solid-state conformations of 18-crown-6 and its complexes. The maps aid in comparisons of related structures, in the perception of pseudo-symmetry elements, and in the classification of the conformations of 18-crown-6. Only four conformational groups are found in the 1 : 1 complexes of 18-crown-6 with sodium, potassium, rubidium, cesium, thallium(I), calcium and strontium cations. The relationship of donor number, mean cavity radius and effective ionic radius combined with skeletal drawings of the donors and the polar map of the torsion angles provide a composite picture of the structures and insight into the balance between cation-donor interaction energy and conformational energy.

Key words. 18-crown-6, conformations, solid-state complexes, torsion angle.

1. Introduction

Crown ethers and conformations – the two have been tied from Pedersen's first report [1]. Even the 'crown' nomenclature suggests a particular molecular shape. Pedersen was always careful to point out that "some of the molecules might resemble the drawings, [but] they are not intended to represent their actual conformations" [1]. Even so, it is clear that he believed from the beginning that the 18-crown-6 ring system would adopt a 'crown' conformation as implied from planar drawings [2, 3].

The first X-ray structures of crown ether complexes [4], showed that Pedersen's caution was warranted: dibenzo-18-crown-6 forms a 'shallow cup' for cations, and dibenzo-24-crown-8 twists to encircle two potassium ions. An ideal 'crown' conformation was first reported by Dunitz, Dobler and their co-workers in 1974 [5] as found in the K^+, Rb^+ and Cs^+ complexes of unsubstituted 18-crown-6. They also reported the C_i conformation for the free ligand, and an 'irregular conformation' for the Na^+ complex [5]. But it is the highly symmetric, D_{3d} conformation that immediately became the paradigm of crown ether conformations.

Crown ether conformations control the complexation reactions. Thermodynamic stability is enhanced when the ligand is 'preorganized' to reduce the energy of

This paper is dedicated to the memory of the late Dr C. J. Pedersen.

reorganization [6]. Kinetic barriers to complexation are principally due to conformational changes which precede interactions with cations [7]. Thus control of ligand conformation, by use of conformationally defined sub-units, has become a standard feature in the design of new complexing agents [8].

Inherent conformational properties are important, but for flexible ligands such as crown ethers, 'the guest organizes the host' [9]. This is seen in the solid-state structures of lariat ethers [10] and of polycarboxylate crown ethers derived from (+)-tartaric acid [11]. In such cases, the ligand mean cavity radius adapts to match the effective ionic radius of the guest. The host optimizes the number of donors to the cation and alters its conformation to best surround different guest cations.

Although the D_{3d} conformation is commonly observed in the solid-state structures of 18-crown-6 and its derivatives, 'irregular' conformations are not rare. Even among the 'irregular' conformations there are marked conformational regularities. The ethylenedioxy units show a preference for an *anti, gauche, anti* sequence of torsion angles for the bonds of the —O—C—C—O— unit [4, 12, 13]. Additional substituents with well defined conformational preferences, such as *R,R*-(+)-tartaric acid, reinforce the preference for a *gauche* relationship between oxygens [14]. Yet even in such conformationally restricted cases, 'irregular' conformations are common [11].

Our goal in this paper is to explore the conformations found in the solid-state structures of 18-crown-6 and its derivatives with special emphasis on 'irregular' or distorted conformations. We outline a procedure for displaying torsion angle information in a form that permits immediate recognition of similarities and differences between related structures. We will show that there are four main groups of conformations, each with its own defined donor array for binding cationic guests. The idea of 'irregular' conformation will be replaced by a proposal for the perception and naming of conformational regularities. We will then examine the solid-state complexes of 18-crown-6, and will show that although the guest certainly organizes the host, the conformational preferences of the host are completely respected.

2. Polar Maps of Endocyclic Torsion Angles

A specific conformation of 18-crown-6 is defined by the 18 endocyclic torsion angles and the C—C and C—O bond lengths. The bond lengths vary little [5, 12, 13] and the torsion angles cluster about $\pm 60°$ (O—C—C—O) and 180° (C—O—C—C). Stoddart [14] and Dale [15] exploited these regularities to define idealized 'bird's-eye' perspective drawings to represent conformations of macrocycles. More recent computer generated perspective and stereo drawings convey the exact conformation of a particular solid-state or molecular mechanics structure. Even so, the *perception* of the conformation, and discovery of its relationship to other conformations is a challenging task. An alternative procedure, discussed in detail by Weiler [16], summarizes the torsion angle information as a map on polar coordinates. The three dimensional perception problem is reduced to *pattern recognition* in two dimensions.

2.1. MAKING A POLAR COORDINATE MAP

Endocyclic torsion angles are determined with the convention that a positive torsion angle exhibits a clockwise rotation between the front and the rear three

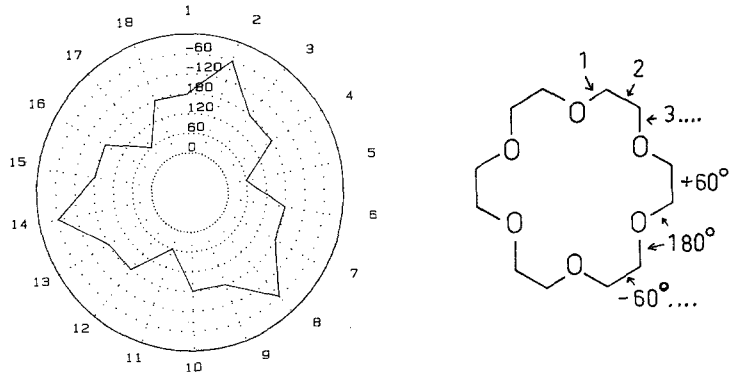

Fig. 1. Polar coordinate map of the torsion angles of an ideal D_{3d} conformation showing the bond numbering convention.

atom planes. The macrocycle *bonds* are numbered sequentially: the starting point and direction can be chosen randomly. The torsion angle of each bond is then plotted by bond number on a polar coordinate system. For 18-crown-6, each bond accounts for 20° (one-eighteenth) of 360°, and the resultant map is an octadecagon. The torsion angles are plotted from the center at 0° to the outer edge (360°); negative torsion angles are plotted as 360° plus the negative torsion angles. This plotting convention differs from Weiler [16], but is useful for crown ethers. It diminishes the small differences about *anti* torsion angles (+175° vs. −175°) and accentuates the equally small differences between *eclipsed* torsion angles (+5° vs. −5°). The former are very common in crown ethers, while the latter occur very rarely [13]. Figure 1 illustrates the procedure for an 'ideal' D_{3d} conformation consisting of torsion angles set to 180° and ±60°. The map, like the actual conformation has three-fold symmetry. The three mirror planes of the map correspond to the three two-fold axes of the D_{3d} symmetry group. The starting point, and direction of bond numbering can be chosen arbitrarily. Rotations and reflections of the resultant map will give equivalent maps for overlay comparisons between structures. Pattern recognition is not impaired by the arbitrary starting point.

2.2. USING POLAR COORDINATE MAPS

One of the uses of the polar coordinate maps is *perception of symmetry elements*. This was alluded to above and will be generally true: a mirror plane in a polar coordinate map will always locate a two-fold rotation axis in the conformation represented by the map [16]. Similarly, perpendicular rotation axes or inversion centers are simply identified. However, some three-dimensional symmetry operations, such as rotation/reflection, S_n, have no two-dimensional counterparts, and the polar map will not assist in perceiving such elements. Real structures are rarely perfectly symmetric. The maps are very useful for detecting pseudo symmetries as individual torsion angles can be selectively ignored while the remaining features are examined.

More importantly, the maps are useful for *comparisons of structures*. For example, the structure of the NaI complex of 2,3,11,12-tetraphenyl 18-crown-6 dihydrate [17] shows the Na^+ ion at the center of the macrocycle, coordinated to

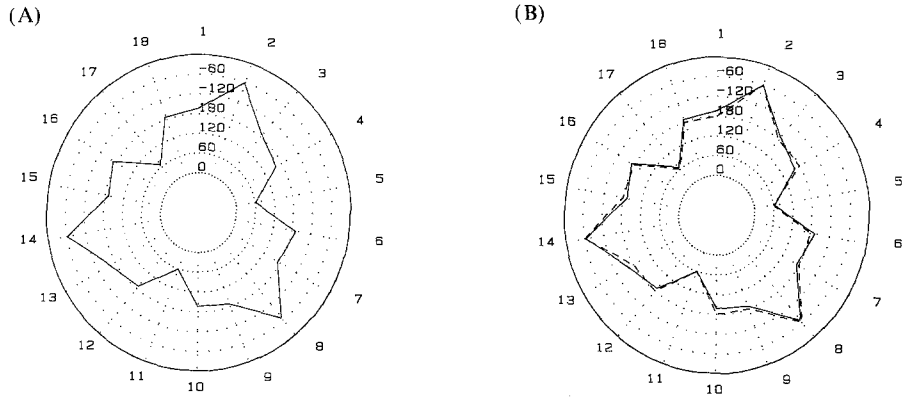

Fig. 2. (A) Polar coordinate map of the torsion angles of the *cis-anti-cis*-2,3,11,12-tetraphenyl-18-crown-6 complex of NaI dihydrate [17,CENPEQ]; (B) Overlay comparison with an "ideal" D_{3d} map (– – –).

two water molecules in axial positions. The water—Na^+—water axis is tilted due to interactions with the phenyl substituents. The polar map of the torsion angles, Figure 2a, is clearly related to the D_{3d} map of Figure 1, with lowered symmetry; compare bonds 3 and 18, which should be mirror images of one another. An overlay of the map with the 'ideal' D_{3d} case is given in Figure 2b. Several minor adjustments of torsion angle, localized in the C—O—C—C units, rather than the O—C—C—O units, can be found. The macrocycle in this structure is pseudo D_{3d}; the maps reveal how the minor distorsions are accommodated.

The central thrust of this paper is an analysis of conformations which are not pseudo-D_{3d}. Consider how the differences can be detected with reference to the maps of Figure 3. Figure 3a refers to the Cs^+ complex of the 18-crown-6 hexaacid derived from three units of *R,R*-(+)-tartaric acid [11]. The map lacks three-fold symmetry, but has an approximate mirror plane through bonds 5 and 14. The

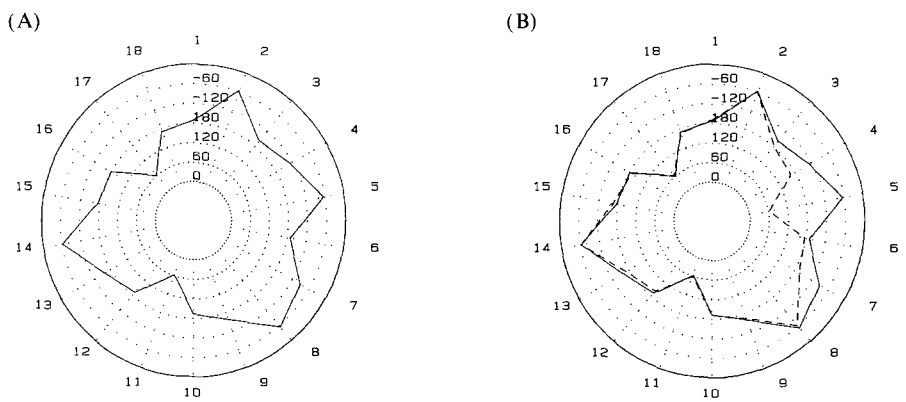

Fig. 3. (A) Polar coordinate map of torsion angles of the Cs^+ salt complex of an 18-crown-6 hexaacid [11]; (B) Overlay comparison of the Cs^+ (——) and Tl^+ (– – –) polar maps of the same ligand.

related Tl^+ complex of the same crown ether is pseudo-D_{3d}. Close inspection of the stereo drawings showed that the two structures differed, but it was difficult to localize the essential differences in the conformation. An overlay of the maps for the Cs^+ and Tl^+ complexes is given in Figure 3b. It is trivial to detect that the principal differences occur in bonds 4, 5 and 7. Bond 5 is an O—C—C—O torsion angle which has switched sign from *gauche*$^+$ in the Tl^+ complex to *gauche*$^-$ in the Cs^+ complex. This is accompanied by changes in C—O—C—C torsion angles at bonds 4 (*anti* to $-128°$) and 7 (*anti* to $-90°$). Reinspection of the structure shows that these motions reorganize the pendent carboxyl groups to enable intermolecular chelation of a Cs^+ ion in an adjacent complex [11].

The essential point in using these maps is that complex information is summarized in a form which draws the chemist's attention to critical substructures. Our uses of the maps have concentrated on analyses of pairs of structures [11, 18], as outlined in the two examples above. This will be possible for any pair of related macrocycles, of any ring size, and will permit easy perception of conformational relationships.

2.3. CONFORMATIONAL GROUPS IN 18-CROWN-6 STRUCTURES

Polar maps can also be used for *perception of groups of conformations*. In our survey of the maps drawn from available crystal structure data, we were struck by recurring patterns in the maps. Some maps, like the Cs^+ example in Figure 3, had pseudo-mirror planes. Others were axially symmetric. Still others lacked any symmetry elements. We were eventually able to recognize six different types of map patterns and symmetries.

The clue to organizing the patterns was provided by the example of Figure 3. The Cs^+ structure is related to the Tl^+ structure by a *gauche*$^+$ to *gauche*$^-$ interconversion in a single ethylenedioxy unit (plus other angle adjustments discussed in detail below). The sequence of the *gauche* torsion angles of the ethylenedioxy units in the Cs^+ structure is $g^+, g^-, g^-, g^-, g^+, g^-$, compared to the D_{3d} sequence $g^+, g^-, g^+, g^-, g^+, g^-$.

We had already generated a map for the 'ideal' D_{3d} conformation with $\pm 60°$ and $180°$ torsion angles (Figure 1). What does the map for the Cs^+ torsion angle sequence look like when 'ideal' values are used? What other sequences of *gauche* torsion angles occur in 18-crown-6 structures? What do the maps of those look like when 'ideal' values are used? The answers are given in Figures 4–6.

There are two sequences involving three positive and three negative torsion angles (Figure 4): the D_{3d} sequences $g^+, g^-, g^+, g^-, g^+, g^-$, (Figure 4a), and another sequence, $g^+, g^-, g^-, g^+, g^+, g^-$, given in Figure 4b. There are four sequences involving four torsion angles of like sign and two torsion angles of opposite sign. They occur in pairs, as the sequences $g^+, g^-, g^-, g^-, g^+, g^-$, (as in the Cs^+ structure of Figure 3, 'ideal' map Figure 5a), and $g^-, g^+, g^+, g^+, g^-, g^+$, (Figure 5b) are enantiomers. The maps of the remaining sequence $(g^+, g^-, g^-, g^+, g^-, g^-,)$ and its enantiomer $(g^-, g^+, g^+, g^-, g^+, g^+,)$ are given in Figure 6.

Two points require comment. Firstly, these torsion angle sequences are the ones that *commonly* occur. The coverage of our analysis is given in Section 2 and

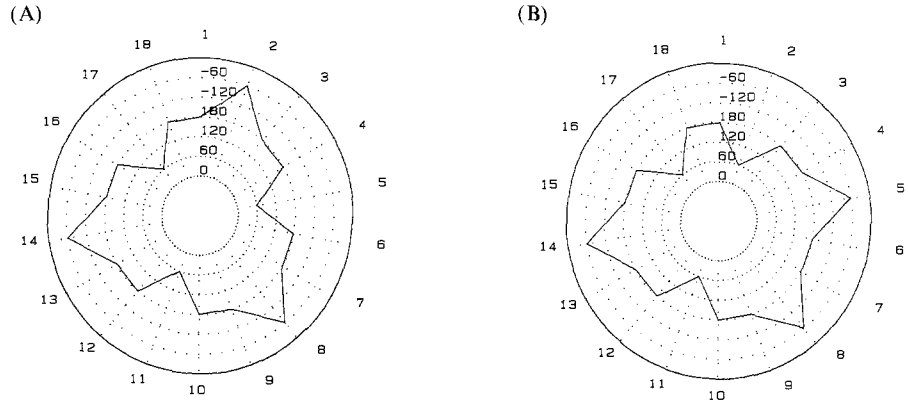

Fig. 4. Polar coordinate map of torsion angles of 'ideal' conformations: (A) D_{3d}; (B) $S_2(g^+, g^+, g^-, g^+, g^-, g^-)$.

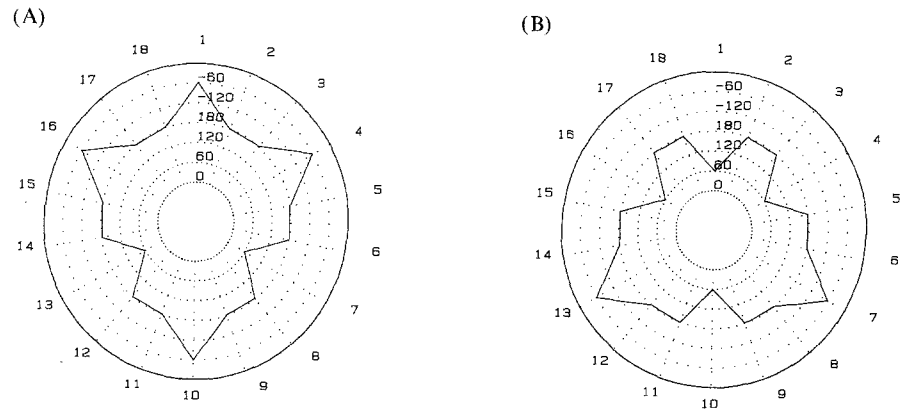

Fig. 5. Polar coordinate map of torsion angles of 'ideal' conformations: (A) $C_2(g^+, g^-, g^-, g^-, g^+, g^-)$; (B) $C_2(E^+)(g^-, g^+, g^+, g^+, g^-, g^+)$.

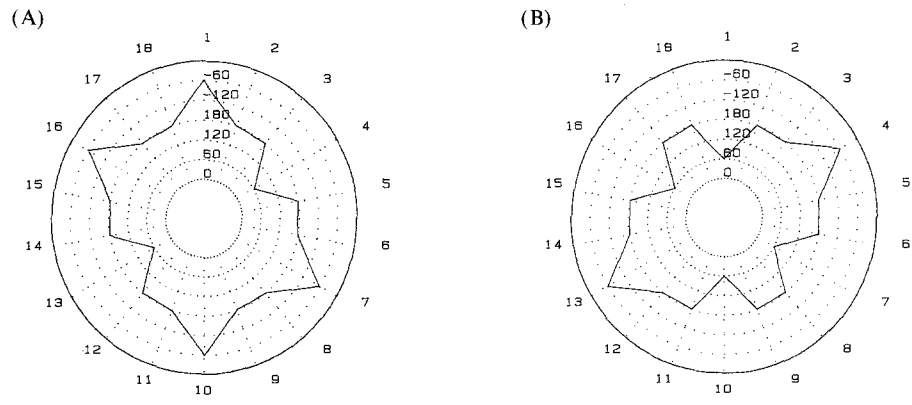

Fig. 6. Polar coordinate map of torsion angles of 'ideal' conformations: (*A*) $C_2(A-)(g^+, g^-, g^-, g^+, g^-, g^-,)$; (B) $C_2(A+)(g^-, g^+, g^+, g^-, g^+, g^+)$.

examples drawn from real structures are discussed. There are several other combinations of signs for the *gauche* O—C—C—O units that can be written ($g^+, g^+, g^-, g^-, g^-, g^-$, for example), but real examples were not found within the group considered.

Secondly, the maps of the pairs of enantiomers are not mirror images of one another. This is an artifact of the plotting convention. The Weiler convention [16] places $+180°$ at the center and $-180°$ at the other edge and gives the result that enantiomeric maps will be superimposible by rotation. As noted above, we choose to minimize the difference about the *anti* torsion angles, with the result that maps of enantiomers are different. The symmetry elements in the plane are the same for the two enantiomers. Both maps of Figure 5 have a single mirror plane; both maps of Figure 6 have two mirror planes. These planes correspond to C_2 axes in the structures.

The 'ideal' maps illustrated define conformational regularities in 18-crown-6 structures. We propose to name the conformations found in real structures by matching the experimental torsion angle map to one of the ideal cases illustrated in Figures 4–6. This is current practice for pseudo-D_{3d} cases, such as Figure 2, and it will be possible for other map patterns as well. Our naming proposal draws on the symmetry elements of the 'ideal' cases. Both enantiomeric sets in Figures 5 and 6 display C_2 axes, but the axes differ in orientation. The Figure 5 axis lies in the plane of the macrocycle, while the Figure 6 axes include one perpendicular to the plane of the macrocycle. The groups are named accordingly: Figure 5 defines the group $C_2(E)$ (for an equatorial C_2 axis) and Figure 6 defines the group $C_2(A)$ (for an axial C_2 axis). Within each group, the enantiomers are distinguished by the sign of the *gauche* angle in excess i.e. $g^+, g^-, g^-, g^-, g^+, g^-$, Figure 5a, is $C_2(A-)$ and its enantiomer is $C_2(A+)$.

The remaining group (Figure 4b) is defined as S_2 as the real structures in this class display a pseudo-rotation reflection axis. Note that S_2 *structures* cannot exist as enantiomers, but the *maps* lack a plane symmetry element and therefore could appear as mirror images. This is another artifact of the plotting conventions: the two different numbering directions will result in mirror image maps from a single structure of S_2 symmetry. The perception of the S_2 class is not impaired by this artifact, and rotation/inversion of the map will lead to maps of the same handedness for overlay comparisons.

The pseudo symmetries of the groups can be discerned in the stereo pairs given in Figure 7. The 18-crown-6 conformation are excised from X-ray structures of examples of each class. The $C_2(A)$ and $C_2(E)$ structures have an excess of *gauche*$^-$ torsion angles i.e. they are $C_2(A-)$ and $C_2(E-)$.

Recall that a sign change in one of the *gauche* torsion angles converted the hexaacid Tl^+ structure (D_{3d}) to the Cs^+ structure ($C_2(E-)$, Figure 3). The other groups are similarly related by single *gauche* sign changes. The interconversion relationships are illustrated in Figure 8. These could represent interconversion pathways for 18-crown-6 in solution [15]. We use them for describing structures near the limit of one group as a 'transition' structure between two pseudo-symmetry classes. This is illustrated in Figure 9 for the Sr^{2+} complex of the *anti*-diastereomer of an 18-crown-6 diacid dianilide [19]. The conformation lies near the extreme of S_2, with significant deviations at bonds 6 and 17. The latter is a regular feature,

discussed in the next section; the former is a striking deviation from typical values ($-1°$, nearly perfectly *eclipsed*). Had this angle distorted even further to 5°, the map would then be an extreme of the $C_2(A+)$ group (Figure 9b).

2.4. 'IDEAL' VS. REAL CONFORMATIONS

The 'ideal' maps of Figures 4–6 were generated by assuming that the macrocycle could achieve $\pm 60°$ and 180° torsion angles in a prescribed sequence. Unfortu-

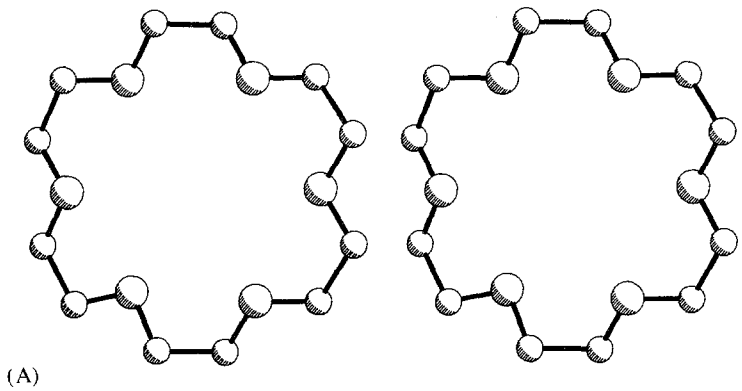

(A)

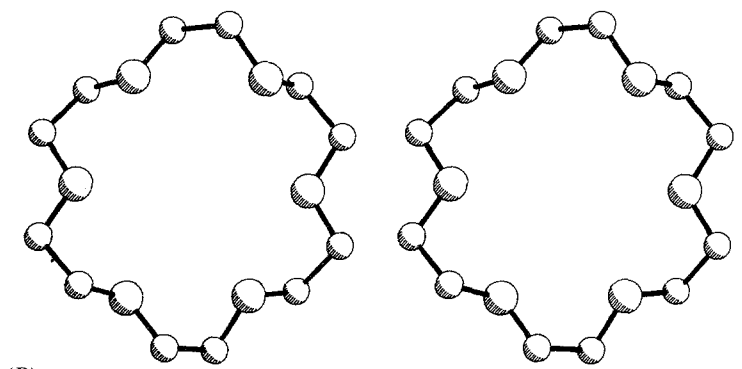

(B)

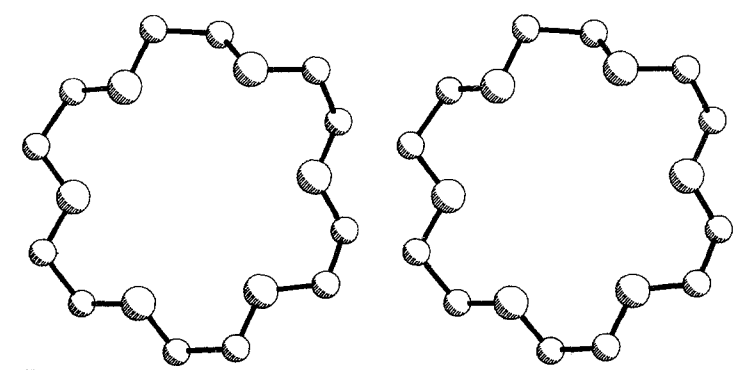

(C)

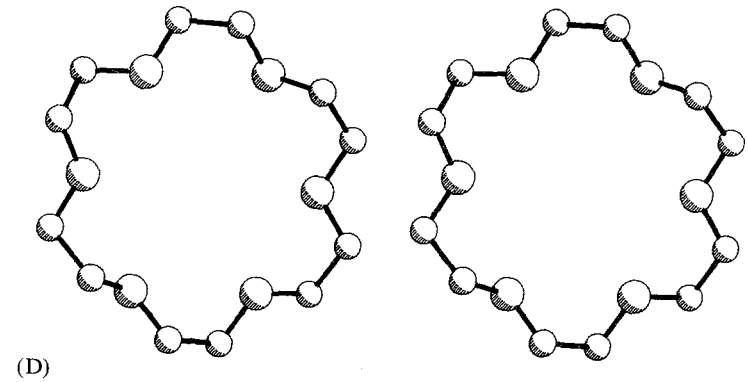

Fig. 7. Stereo drawings of 18-crown-6 conformations taken from representative structures: (A) D_{3d} (HEXH); (B) S_2 (TETNA); (C) $C_2(E-)$(HEXCS); (D) $C_2(A-)$ (TETCS).

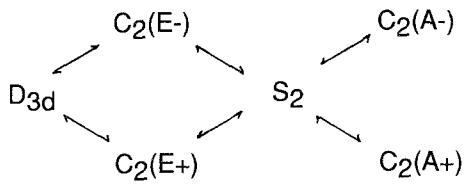

Fig. 8. Interconversions between conformational groups produced by single *gauche*$^+$ to *gauche*$^-$ changes in the O—C—C—O torsion angles.

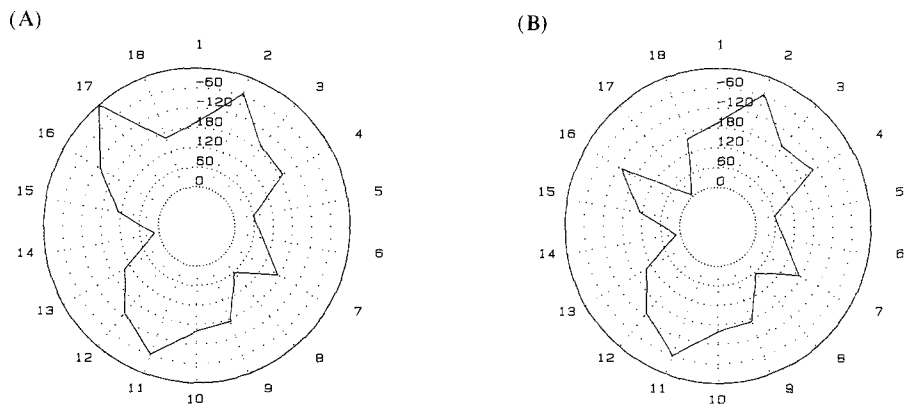

Fig. 9. (A) Polar coordinate map of the torsion angles of CAHXOB illustrating an extreme of the S_2 conformational group. (B) torsion angle map of CAHXOB with bond 17 switched from $-1°$ to $+5°$, illustrating an extreme of the $C_2(A+)$ conformational group.

nately this is not physically realistic. We 'built' and optimized the bond lengths and bond angles of an oligoethylene glycol chain using a molecular mechanics package [20], and then imposed the 'ideal' torsion angles on the chain using the torsion angle input features of the program. The distance from the first to the seventh oxygen was determined. For an 'ideal' D_{3d} sequence, the separation was zero, as expected. For the other groups, the separation was 610–640 pm, clearly indicating that the 'ideal' conformation cannot exist. Distorsions are inevitable. A close inspection of the maps of real conformations, in overlap with their 'ideal', shows that the main distorsions are localized in key regions. When these key distorsions are included in the molecular model, the first and seventh oxygens approach to within 30 pm.

The structure used for the stereoscopic drawing of the S_2 class is the Na^+ salt complex of the 18-crown-6 tetraacid derived from two tartaric acid units [11]. The map and its overlay with the 'ideal' S_2 map are given in Figure 10. The main difference in torsion angle between the two structures is at bond 1 (using the orientation of the 'ideal' map as illustrated in Figures 4 and 10b). The 'ideal' *anti* torsion angle for a C—O—C—C unit is 90° in the real structure [11]. The same bond in the map in Figure 9, also S_2 (bond 6), is 86°. From molecular modelling, a value between 75° and 105° brings the first and seventh oxygens to within 50 pm of one another, with the closest approach at 90°. Not just any distortion from 'ideal' will work to bring the ends close; *only distorsions of bond 1 will close the macrocycle*. All the examples in this class exhibit distortion and closely overlay the map in Figure 10 (or its mirror image) and take values for the bond 1 torsion angle ranging from 73° to 112°.

The other classes behave similarly; there are critical locations for deviation from the 'ideal' values and the deviations take well defined values. In every case, the deviation applied to the molecular model brings the first and seventh oxygens close to one another. Real examples in the two C_2 classes are illustrated in Figures 11 and 12. In general, two or three *gauche* angles of like sign in the O—C—C—O units

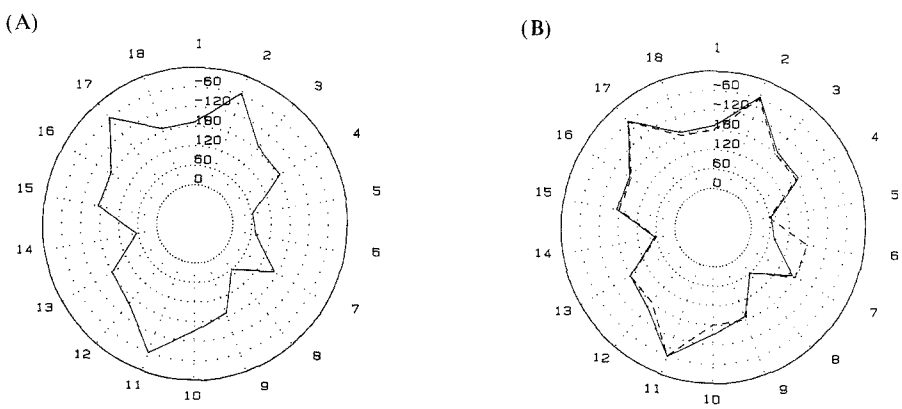

Fig. 10. (A) Polar coordinate map of TETNA torsion angles. (B) Overlay of the TETNA map with an ideal S_2 map. Note the deviation at bond 6. The S_2 map of Figure 4B has been inverted and rotated to overlay the experimental map of Figure 10A.

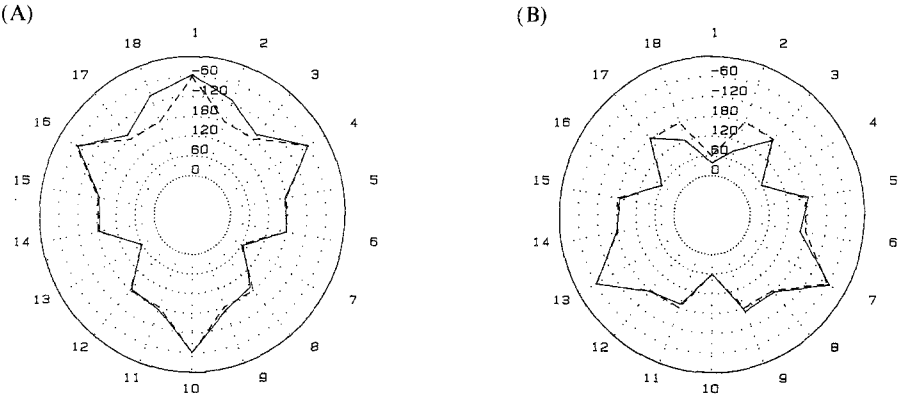

Fig. 11. Comparison of ideal and real polar coordinate maps: (A) Overlay of torsion angle maps of TETH (——) and 'ideal' $C_2(E-)$ (– – –); (B) Overlay of torsion angle maps of NACRWB (——) and 'ideal' $C_2(E+)$ (– – –).

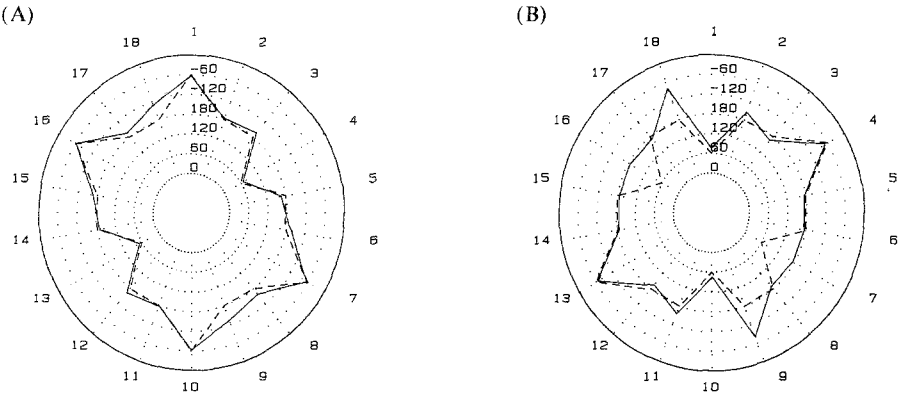

Fig. 12. Comparison of ideal and real polar coordinate maps: (A) Overlay of torsion angle maps of TETCS (——) and 'ideal' $C_2(A-)$ (– – –); (B) Overlay of torsion angle maps of 18C6 (——) and 'ideal' $C_2(A+)$ (– – –).

provoke deviations in the adjacent C—O—C—C units. The distorsions take an *anti* torsion angle to a value about $\pm 90°$.

These are major and systematic 'first-order' adjustments to the zeroth order solution presented by the 'ideal' map. There are small 'second-order' adjustments throughout the structures. These will optimize interactions with guests, relieve strain, improve contacts in the crystal, or achieve any of the other optimizations that are important in the solid state. The value of the pattern recognition approach is that it ignores the minor detail in favor of the larger picture.

It would be possible to redefine 'ideal' to incorporate the additional regular distorsions observed. The resultant maps would then closely resemble the real cases in Figures 10–12. But this is not necessary for pattern recognition purposes. Assigning a structure to one of the conformational groups is easily done by

inspection of the map in conjunction with Figures 4–6. Once an assignment is made, detailed comparison with structures from the same group will reveal how both the systematic, and the specific distorsions from 'ideal' are accommodated.

3. Structures of 18-Crown-6 Complexes in the Solid State

We turn to a survey of the structures of 18-crown-6 complexes in the solid state. A search of the Cambridge Crystallographic Database in August 1988 using '18-crown-6' with Group 1 and 2 cations gave a core of references. Structures with $R > 0.10$, structures in which the crown ether was disordered, and 2:1 or 1:2 complexes were rejected. The remaining structures were supplemented with structures from our own work on 18-crown-6 tetra- and hexa-acids [11]. The final dataset is given in Tables I–III. The set is complete for 18-crown-6 and its derivatives which do not involve ring fusion with the macrocycle (benzo-, cyclohexano-, polycyclic structures). The coverage is similarly complete for Na^+, K^+, Rb^+, Cs^+, Tl^+, Ca^{2+}, Sr^{2+} and Ba^{2+} as single guests. Ammonium salts and neutral guests have not been systematically examined, although a few examples are included in Table III.

Our analysis considers two aspects of the structures. Firstly we consider the coordination geometry about the cation and the relationship of cavity size to the effective ionic radius of the guest cation. For each complex we calculate the mean cavity radius by the procedure of Mathieu *et al.* [21], which averages the differences between the metal–donor distance and the covalent radius of donor oxygen of all donors from the ligand. The mean cavity radius can then be compared to the effective ionic radius of the cation for various coordination numbers [23]. The donor geometry around the cation can be determined from skeletal drawings, and classified by analogy between the six oxygen positions of the 18-crown-6 with the conformations of cyclohexane [10, 11]. These analyses emphasize the coordination from the guest's perspective. The host's perspective is the macrocycle conformation, as revealed by polar maps of torsion angles. Here the host's role in establishing the coordination environment is the issue. We can then compare the macrocycle conformation with the cavity radius and the skeletal donor atom arrangement.

3.1. POTASSIUM 18-CROWN-6 COMPLEXES

The structural data are summarized in Table I and give the overwhelming sense of a close kinship between the complexes. The coordination numbers range from 6 to 9, but the majority of these are accommodated by a D_{3d} macrocyclic conformation. This places the donors in a chair skeletal arrangement. The exceptions are 18-crown-6 tetraamides derived from (+)-tartaric acid [19]. The tartaro units prefer an *anti* conformation of the carboxyl groups [22]; this places the carboxyl substituents in axial positions on the macrocycle and sets a *gauche*$^-$ conformation between the ether oxygens of each tartaro unit [11]. The substituent placement and the conformational preference combine to exclude a D_{3d} conformation. No D_{3d} conformations are found for any of the 18-crown-6 tetraacid complexes; this K^+ structure is not anomalous in that context.

Table I. Summary of K^+ structures[a].

Structure	Conformational Group	Skeletal Configuration	Donor Number	Cavity Radius (Å)	Other Donors
KCROFE	D_{3d}	CH	6	1.37	
CULJOI	D_{3d}	PL/CH	6	1.37	
FAPNAL	D_{3d}	CH	7	1.38	$I(PhSbI_2)_4^-$
BONSAY	$C_2(E-)$	PL	7	1.39	C=O
DECDUK	D_{3d}	CH	7	1.39	W
DEDFUN	D_{3d}	CH	7	1.40	$(SCN)_4Co^-$
KTHOXD	D_{3d}	CH	7	1.40	SCN^-
DEJWOE	D_{3d}	PL/CH	7	1.41	O_2NAr^-
DUMZAM	D_{3d}	CH	7	1.44	NO_3^-
DAXNAR	D_{3d}	CH	7	1.50	$H_3Ru(PPh_3)_3^-$
ClBFEY	D_{3d}	CH	7	1.50	$H\text{-}MoCp_2^-$
DIKXEA	D_{3d}	CH	8	1.41	$Fe_4(AuPEt_3)(CO)_{13}^-$
DIJXOJ	D_{3d}	CH	8	1.41	$P(CN)_2^-$
DIJLAJ	D_{3d}	PL/CH	8	1.41	CuI_2^-
HOXOKM	D_{3d}	CH	8	1.41	W, $Mo_6O_{19}^{2-}$
CEXJIY	D_{3d}	CH	8	1.45	C=O
DEBVUB	D_{3d}	CH	8	1.51	C=O
BONSAY	$C_2(E-)$	PL	8	1.51	C=O
CRKEAC	D_{3d}	CH	8	1.53	$C{=}O^-$
HOXOMK	D_{3d}	CH	8	1.53	W, MoO_4^{2-}
HEXK	D_{3d}	PL	9	1.48	W, CO_2^-, C=O
DEJWUK	D_{3d}	CH	9	1.53	O_2NAr^-, W

[a] Abbreviations: CH = chair; PL = planar; TW BT = twist boat; BT = boat; HF CH = half chair; RE CH = rectangular chair; * = no group assigned; W = water; THF = tetrahydrofuran.

The range of cavity size for a given donor number is larger than anticipated by an earlier analysis [10]. The group averages of cavity radius (*CR*) compare well with the K^+ effective ionic radii (*IR*) for different donor numbers [23]: 6 coord., $CR = 137$ pm, $IR = 138$ pm; 7 coord., $CR = 142$ pm, $IR = 146$ pm; 8 coord., $CR = 147$ pm, $IR = 151$ pm; 9 coord, $CR = 151$ pm, $IR = 155$ pm. In general, smaller cavity radii than expected are associated with soft, highly delocalized donors contributed by the counterion. The Shannon ionic radii were derived from oxide and chalconide structures and thus would apply best to hard donor sites [23]. A soft donor to K^+ would require the crown ether sites to compensate with increased interaction and shorter donor-cation separations. Larger cavity radii than expected (DAXNAR [24] and CIBFEY [25]) are associated with very large counterions that block potential sites for additional donors without actually contributing a formal donor atom for the K^+. Both these structures also involve a metal hydride coordinated to K^+. There are too few examples to generalize further on factors leading to larger cavity sizes.

There is no Relationship Between the Conformational Symmetry and the Cavity Size. In K^+ complexes, D_{3d} can contract to 137 pm and expand to 153 pm. The changes are accommodated by minor adjustments in the *anti* torsion angles of the C—O—C—C fragments as discussed above (Figure 2). There is a relationship between the D_{3d} conformational group and the chair skeletal arrangement; only D_{3d} gives the chair donor atom set.

3.2. SODIUM 18-CROWN-6 COMPLEXES

The sodium complexes, summarized in Table II, show a much broader spectrum of structures. The cavity sizes range from 113 pm to 137 pm and follow the donor

Table II. Summary of Na^+ structures (see Table I for abbreviations).

Structure	Conformational group	Skeletal Congfiguration	Donor Number	Cavity Radius (Å)	Other Donors
DIDCEY	*	BT	6	1.13	
NATHOD	$C_2(E+)$	BT	7	1.15	W
TETNA	S_2	TW BT	7	1.16	C=O
CENPOA	S_2	HF CH	7	1.16	I^-
NACRWB	$C_2(E+)$	HF CH	8	1.23	$W_2(CO)_{10}SH^-$
HEXNA	D_{3d}	PL	8	1.28	$W CO_2^-$
BOYYUJ	D_{3d}	CH	8	1.34	THF
NACRWA	D_{3d}	Pl CH	8	1.35	$W(CO)_5SH^-$
NACNPB	D_{3d}	CH	8	1.36	THF
XOCCPN	D_{3d}	PL CH	8	1.36	THF
CENPEQ	D_{3d}	CH	8	1.36	W
NACNPA	D_{3d}	CH	8	1.37	THF

numbers. However, the cavity radii are consistently larger than the effective ionic radii [23]; 6 coord., $CR = 113$ pm, $IR = 102$ pm; 7 coord., $CR = 116$ pm, $IR = 112$ pm; 8 coord., $CR = 130$ pm, $IR = 118$ pm. 18-Crown-6 is indeed 'too large for Na^+', even though the cavity size can adapt through a large range. This is the sign that the macrocycle is not completely flexible, nor can it be completely organized by the guest cation. Truter [4] suggests that these larger Na^+—O distances result from all potential donors of the macrocycle interacting with the cation. In other words, the macrocycle *enforces* a high coordination number for the complex. D_{3d} conformations giving chair or planar donor skeletal arrangements are associated with the larger cavity radii found in the 8 coordinate complexes. As the donor number and the cavity radius decreases, the skeletal array adopts half chair, twist boat and ultimately boat arrangements to permit shorter Na^+—O contacts. This is an energy balance between the Na^+—O interaction and the conformational energy of the macrocycle. The energy to achieve a conformation with shorter Na^+—O contacts must be too large, because the observed cavity radii are consistently larger than the effective ionic radii.

The K^+ structures suggested that soft donor sites would lead to closer cation–macrocycle contacts, and smaller cavity sizes. A similar effect is found in the Na^+ data (NACRWB [26]), but the data set is too small to establish a trend. The DIDCEY structure [27] represents an extreme for Na^+ to 18-crown-6 interaction. The counterion is a bis-mercapto Fe(III) tetraphenylporphyrin complex which has no localized donor site for additional interaction with the Na^+. Consequently, the 18-crown-6 must provide the full stabilization for the cation. The macrocycle is distorted to the point where none of the conformational groups is appropriate to describe the conformation (Figure 13). This may be an example of a conformational group derived from four consecutive O—C—C—O torsion angles of like sign followed by two of the opposite sign, but the 'ideal' map is so remote that generalization is not warranted. The DIDCEY structure represents an uneasy compromise between the conformational energy of the 18-crown-6 and the Na^+—O interaction. Crystal packing might play a significant role in such a balanced system.

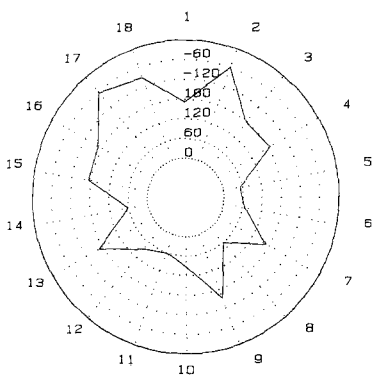

Fig. 13. Polar coordinate map of the torsion angles of DIDCEY [27].

3.3. OTHER 18-CROWN-6 COMPLEXES

The remaining complexes are summarized in Table III. The data set for any cation is too small to permit generalizations, but the main themes developed above can be detected. Donor number and cavity size are related, and the effective ionic radii of the guests follow the cavity radii closely. The ideal D_{3d} conformation is poorly represented, but when it occurs, the skeletal donor array is in a chair arrangement. There is no relationship between any other conformational group and a particular skeletal array.

4. Extensions and Exceptions

Exceptions? By definition there will be exceptions [28]. The DIDCEY structure discussed above is one example. There will always be exceptions to any procedure that attempts to describe a real system using idealized limiting structures. It is precisely the deviations from ideality that provide the most insight into the molecular recognition process in the structures discussed.

There are certainly other 18-crown-6 structures with polar coordinate maps which do not fall within the classes defined above. Our coverage excluded 2:1 complexes, with hydrogen bonding guests, 18-crown-6 fused to additional rings etc. There may well be additional regularities among the excluded structures. The *perception* of those regularities will certainly be aided by the polar maping procedure outlined here.

We have not explored the question of relative energy of the various conformational groups. Molecular mechanics calculations have established that the solid-state structures of 18-crown-6, and its Na^+ and K^+ complexes are the minimum energy structures [29–31]. The distribution of structures among the conformational groups suggests that the D_{3d} conformation is generally a low energy structure with the other conformational groups somewhat higher in energy. It may be appropriate to extend the skeletal analogy with cyclohexane to include energetics as well; the chair (D_{3d}) in a global well, with several closely related conformations at higher but similar energy. This proposal is supported by the results of Uiterwijk *et al.* [32]. They describe a diamond-lattice method for enumeration of the number of conformation of crown ethers, including 18-crown-6. They then compute relative conformational energies using average values of attractive and repulsive energies. The D_{3d} conformation is a minimum in their analysis; and 'ideal' S_2 conformation lies 9.1 kJ/mol higher while an 'ideal' $C_2(A)$ conformation is 11.7 kJ/mol above D_{3d}. More recently the same group has examined the energetics as a function of dielectric constant [33]. The energy differences between 'ideal' conformation are attenuated for realistic values of dielectric constant, but the conformations examined lie in distinct minima with 'steep walls' [33]. A fuller exploration is warranted.

We have chosen to examine 18-crown-6 structures because these were relevant to our current projects. The polar maps of other macrocycles are easily generated and show interesting patterns. Analogy with cyclohexane may not be appropriate, but there will certainly be more to uncover about conformations and molecular recognition. Polar coordinate maps and cavity size/donor number relationships are the tools for the task.

Table III. Summary of other structures considered (See Table I for abbreviations).

Structure	Guest	Conformational Group	Skeletal Configuration	Donor Number	Cavity Radius (Å)	Other Donors
RBTHXD	Rb^+	D_{3d}	CH	8	1.62	NCS^-
CSTHX	Cs^+	D_{3d}	CH	8	1.74	NCS^-
TETCS	Cs^+	$C_2(A-)$	PL	9	1.76	CO_2^-, W, C=0
HEXCS	Cs^+	$C_2(E-)$	TW BT	10	1.80	CO_2^-, W, C=0
DUBCIM	Cs^+	$C_2(A+)$	TW BT	12	1.95	
TETTL	Tl^+	S_2	HF CH	8	1.61	CO_2^-, C=0
HEXTL	Tl^+	D_{3d}	PL	10	1.61	CO_2^-, W, C=0
CAHXOA	Ca^{2+}	S_2	TW BT	9	1.37	CO_2–, W
DUJJOH	Ca^{2+}	$C_2(A+)$	TW BT	10	1.12	NO_3^-
CAHXOB	Sr^{2+}	$C_2(A-)$	PL	9	1.47	CO_2^-, Cl^-
TETH	W	$C_2(P-)$	HF CH			
HEXH	W_2	D_{3d}	CH			
18C6	NONE	$C_2 2(A+)$	RE CH			
SUCCIN	$(HO_2CCH_2)_2$	$C_2 2(A+)$	TW BT			
TETEN	$(^+H_3NCH_2)_2$	$C_2(A-)$	TW BT			

Acknowledgement

The ongoing support of the Natural Sciences and Engineering Research Council is gratefully acknowledged.

References

1. C. J. Pedersen: *J. Am. Chem. Soc.* **89**, 7017 (1967).
2. C. J. Pedersen and H. K. Frensdorff: *Angew. Chem. Int. Edn. Engl.* **11**, 16 (1972).
3. C. J. Pedersen: *Science* **241**, 536 (1988).
4. M. R. Truter: *Struct. Bonding* **16**, 71 (1973).
5. J. D. Dunitz, M. Dobler, P. Seiler and R. P. Phizackerley: *Acta Crystallogr.* **B30**, 2733 (1974).
6. (a) R. M. Izatt, D. J. Eatough, and J. J. Christensen: *Struct. Bonding* **16**, 161 (1973); (b) R. M. Izatt, J. S. Bradshaw, S. A. Nielsen, J. D. Lamb and J. J. Christensen: *Chem. Rev.* **85**, 271 (1985); (c) L. F. Lindoy: *The Chemistry of Macrocyclic Ligand Complexes*, Cambridge University Press, 1989.
7. (a) P. B. Chock: *Proc. Natl. Acad. Sci. U.S.A.* **69**, 1939 (1972); (b) C. C. Chen and S. Petrucci: *J. Phys. Chem.* **86**, 2601 (1982); (c) Ref. [6b].
8. (a) J. M. Lehn: *Struct. Bonding* **16**, 1 (1973); (b) D. J. Cram: *Angew. Chem. Int. Edn.* **25**, 1039 (1986).
9. D. J. Cram and K. N. Trueblood: *Top. Curr. Chem.* **98**, 43 (1981).
10. R. D. Gandour, F. R. Fronczek, V. J. Gatto, C. Minganti, R. A. Schultz, B. D. White, K. A. Arnold, A. D. Mazzocchi, S. R. Miller and G. W. Gokel: *J. Am. Chem. Soc.* **108**, 4078 (1986).
11. P. J. Dutton, T. M. Fyles and S. J. McDermid: *Can. J. Chem.* **66**, 1097 (1988); P. J. Dutton, F. R. Fronczek, T. M. Fyles and R. D. Gandour, crystal structures of TETH and HEXH *J. Am. Chem. Soc.*, **112**, 8984 (1990); crystal structures of salt complexes submitted.
12. M. Dobler: *Ionophores and Their Structures*, Wiley & Sons, (1981).
13. L. Parentau and F. Brisse: *Can. J. Chem.* **67**, 1293 (1989).
14. J. F. Stoddart: *Quart. Rev.* **8**, 85 (1979).
15. J. Dale: *Top. Stereochem.* **9**, 199 (1977).
16. J. P. Ounsworth and L. Weiler: *J. Chem. Ed.* **64**, 568 (1987).
17. G. Weber, G. M. Sheldrick, T. Burgemeister, F. Dietl, A. Mannschreck and A. Merz: *Tetrahedron* **40**, 855 (1984).
18. F. R. Fronczek, T. M. Fyles, R. D. Gandour, P. J. Hocking and P. D. Wotton: *Can. J. Chem.* **69**, 12 (1991).
19. J. P. Behr, J. M. Lehn, D. Moras and J. C. Thierry: *J. Am. Chem. Soc.* **103**, 701 (1981).
20. J. J. Gajewski and W. K. Gilbert: *PC Model*, Serena Software, Bloomington, Indiana.
21. F. Mathieu, B. Metz, D. Moras, R. Weiss: *J. Am. Chem. Soc.* **100**, 4412 (1978).
22. J. Gawronski, K. Gawronska and U. Rychlewska: *Tetrahedron Lett.* **30**, 6071 (1989) and references therein; M. Egli and M. Dobler: *Helv. Chim. Acta* **72**, 1136 (1989).
23. R. D. Shannon: *Acta Crystallogr.* **A32**, 751 (1976).
24. A. S. C. Chan and H. S. Shieh: *J. Chem. Soc., Chem. Commun.* 1378 (1985).
25. J. A. Bandy, A. Berry, M. H. Green, R. N. Perutz, K. Prout, and J. N. Verpeaux: *J. Chem. Soc., Chem. Commun.* 729 (1984).
26. M. K. Cooper, P. A. Duckworth, K. Hendrick and M. McPartlin: *J. Chem. Soc., Dalton Trans.* 2357 (1981).
27. P. Doppelt, J. Fischer and R. Wiess: *Croat. Chem. Acta* **57**, 507 (1984).
28. R. B. Woodward and R. Hoffman: *The Conservation of Orbital Symmetry*, Verlag Chemie, Weinheim (1970), p. 173.
29. R. Perrin, C. Decoret, G. Bertholon and R. Lamartine: *Nouv. J. Chim.* **7**, 263 (1983).
30. G. Wipff, P. Weiner and P. Kollman: *J. Am. Chem. Soc.* **104**, 3249 (1982).
31. G. Ranghino, S. Romano, J. M. Lehn and G. Wipff: *J. Am. Chem. Soc.* **107**, 7873 (1985).
32. J. W. H. M. Uiterwijk, S. Harkema, B. W. van de Waal, F. Gobel and H. T. M. Nibbeling: *J. Chem. Soc., Perkin Trans. 2* 1843 (1983).
33. J. W. H. M. Uiterwijk, S. Harkema, and D. Feil: *J. Chem. Soc., Perkin Trans. 2* 721 (1987).

Crystal Structure References

18C6 $C_{12}H_{24}O_6$; J. D. Dunitz and P. Seiler: *Acta Crystallogr.* **B30**, 2739 (1974).

BONSAY $2(C_{24}H_{44}N_4O_{10}) \cdot 3KBr \cdot 7H_2O$; A.-C. Dock, D. Moras, J.-P. Behr and J.-M. Lehn: *Acta Crystallogr.* **C39**, 1001 (1983).

BOYYUJ $C_{12}H_{24}O_6 \cdot Na^+ \cdot (Nb(C_{14}H_{12})(C_5H_5)_2^-) \cdot 2(C_4H_8O)$; S. I. Bailey, L. M. Engelhardt, W.-P. Leung, C. L. Rastom, I. M. Ritchie and A. H. White: *J. Chem. Soc., Dalton Trans.* 1747 (1985).

CAHXOA $C_{28}H_{32}N_2O_{12}^{2-} \cdot Ca^{2+} \cdot 3H_2O$; J.-P. Behr. J.-M. Lehn, D. Moras and J.-C. Thierry: *J. Am. Chem. Soc.* **103**, 701 (1981).

CAHXOB $C_{28}H_{32}N_2O_{12}^{2-} \cdot Ca^{2+} \cdot 2Cl^-$; J.-P. Behr, J.-M. Lehn, D. Moras and J.-C. Thierry: *J. Am. Chem. Soc.* **103**, 701 (1981).

CENPEQ $C_{36}H_{40}O_6 \cdot NaI \cdot 2H_2O \cdot CH_2Cl_2$; G. Weber, G. M. Sheldrick, T. Burgemeister, F. Dietl, A. Mannschreck and A. Merz: *Tetrahedron* **40**, 855 (1984).

CENPOA $C_{36}H_{40}O_6 \cdot NaI$; G. Weber, G. M. Sheldrick, T. Burgemeister, F. Dietl, A. Mannschreck and A. Merz: *Tetrahedron* **40**, 855 (1984).

CEXJIY $C_{12}H_{24}O_6 \cdot K^+ \cdot C_8H_4O_2P$; C. L. Liotta, M. L. McLaughlin, D. G. Van Derveer and B. A. O'Brien: *Tetrahedron Lett.* **25**, 1665 (1984).

CIBFEY $C_{12}H_{24}O_6 \cdot K^+ \cdot (Mo(C_5H_5)_2H^-)$; J. A. Bandy, A. Berry, M. L. H. Green, R. N. Perutz, K. Prout and J.-N. Verpeaux: *J. Chem. Soc., Chem. Commun.* 729 (1984).

CRKEAC $C_{12}H_{24}O_6 \cdot K^+ \cdot C_6H_9O_3^-$; C. Cambillau, G. Bram, G. Corset, C. Riche and C. Pascard-Billy: *Tetrahedron* **34**, 2675 (1978).

CSTHX $C_{12}H_{24}O_6 \cdot CsNCS$; M. Dobler and R. P. Phizackerley: *Acta Crystallogr.* **B30**, 2748 (1974).

CULJOI $C_{12}H_{24}O_6 \cdot K^+ \cdot C_{19}Cl_{15}^-$; C. Miravitilles, E. Molins, X. Solans, G. Germain and J. P. DeClerq: *J. Incl. Phenom.* **3**, 27 (1985).

DAXNAR $C_{12}H_{24}O_6 \cdot K^+ \cdot (H_3Ru(P(C_6H_5)_3)_3^-)$; A. S. C. Chan and H.-S. Sheih: *J. Chem. Soc., Chem. Commun.* 1378 (1985).

DEBVUB $2(C_{12}H_{24}O_6 \cdot K^+) \cdot Cu^{2+} \cdot 2(S_2C_2O_2^{2-})$; M. G. Kanatzidis, N. C. Baenziger and D. Coucouvanis: *Inorg. Chem.* **24**, 2680 (1985).

DECDUK $C_{12}H_{24}O_6 \cdot K^+ \cdot (closo\text{-}(P(C_6H_5)_3)_2 \cdot RhC_2B_9H_{11}^-)$; J. A. Walker, C. B. Knobler and M. F. Hawthorn: *Inorg. Chem.* **24**, 2688 (1985).

DEDFUN $(C_{12}H_{24}O_6 \cdot K^+)_2 \cdot (Co(SCN)_4^{2-})$; Y. Fan, Z. Zhou, X. Wang, J. Zhang and J. Han: *Kexue Tonbao* **30**, 910 (1985).

DEJWOE $C_{12}H_{24}O_6 \cdot K^+ \cdot C_{12}N_3O_9^-$; M. P. Egorov, V. K. Bel'skii, E. S. Petrov, M. I. Terekhova and I. P. Beletskaya: *Zh. Org. Khim.* **20**, 1855 (1984).

DEJWUK $C_{12}H_{24}O_6 \cdot K^+ \cdot C_{12}N_3O_9^- \cdot 2H_2O$; M. P. Egorov, V. K. Bel'skii, E. S. Petrov, M. I. Terekhova and I. P. Beletskaya: *Zh. Org. Khim.* **20**, 1855 (1984).

DIDCEY $C_{12}H_{24}O_6 \cdot Na^+ + \cdot (C_{44}H_{28}N_4Fe(SC_6HF_4)_2^-) \cdot C_6H_6$; P. Doppelt, J. Fischer and R. Weiss: *Croat. Chem. Acta* **57**, 507 (1984).

DIJLAJ $C_{12}H_{24}O_6 \cdot K^+ \cdot CuI_2^-$; N. P. Rath and E. M. Holt: *J. Chem. Soc., Chem. Commun.* 311 (1986).

DIJXOJ $C_{12}H_{24}O_6 \cdot K^+ \cdot (P(CN)_2^-)$; A. Schmidtpeter, G. Burget, F. Zwaschka and W. S. Sheldrick: *Z. Anorg. Allg. Chem.* **527**, 17 (1985).

DIKXEA $C_{12}H_{24}O_6 \cdot K^+ \cdot (Fe_4(AuP(C_2H_5)_3)(CO)_{13}^-) \cdot CH_2Cl_2$; C. P. Horowitz, E. M. Holt, C. P. Brock and D. F. Shriver: *J. Am. Chem. Soc.* **107**, 8136 (1985).

DUBCIM $(C_{12}H_{24}O_6)_2 \cdot Cs^+ \cdot e^-$; S. B. Dawes, D. L. Ward, R. H. Huang and J. L. Dye: *J. Am. Chem. Soc.* **108**, 3534 (1986).

DUJJOH $C_{16}H_{32}O_6 \cdot Ca(NO_3)_2$; R. B. Dyer, D. H. Metcalf, R. G. Ghirardelli, R. A. Palmer and E. M. Holt: *J. Am. Chem. Soc.* **108**, 3621 (1986).

DUMZAM $C_{14}H_{24}O_6 \cdot KNO_3$; R. B. Dyer, R. G. Ghirardelli, R. A. Palmer and E. M. Holt: *Inorg. Chem.* **25**, 3184 (1986).

FAPNAL $C_{12}H_{24}O_6 \cdot K^+((C_6H_5SbI)_4I^-)$; J. von Seyerl, O. Scheidsteger, H. Berke and G. Huttner: *J. Organomet. Chem.* **311**, 85 (1986).

HEXCS $C_{18}H_{23}O_{18}^- \cdot 2H_2O$; P. J. Dutton, F. R. Fronczek, T. M. Fyles, R. D. Gandour and V. V. Suresh: submitted.

HEXH $C_{18}H_{24}O_{18} \cdot 4H_2O$; P. J. Dutton, F. R. Fronczek, T. M. Fyles and R. D. Gandour: *J. Am. Chem. Soc.* **112**, 8984 (1990).

HEXK $C_{18}H_{23}O_{18}^{-} \cdot K^{+} \cdot 3H_2O$; P. J. Dutton, F. R. Fronczek, T. M. Fyles, R. D. Gandour and V. V. Suresh: submitted.

HEXNA $C_{18}H_{23}O_{18}^{-} \cdot Na^{+} \cdot 3H_2O$; P. J. Dutton, F. R. Fronczek, T. M. Fyles, R. D. Gandour and V. V. Suresh: submitted.

HEXTL $C_{18}H_{23}O_{18}^{-} \cdot Tl^{+} \cdot 2H_2O$; P. J. Dutton, F. R. Fronczek, T. M. Fyles, R. D. Gandour and V. V. Suresh: submitted.

HOXOKM $(C_{12}H_{24}O_6 \cdot K^{+})_2 \cdot Mo_6O_{19}^{2-} \cdot H_2O$; O. Nagano and Y. Sasaki: *Acta Crystallogr.* **B35**, 2387 (1979).

HOXOMK $(C_{12}H_{24}O_6 \cdot K^{+})_2 \cdot MoO_4^{2-} \cdot 5H_2O$; O. Nagano: *Acta Crystallogr.* **B35**, 465 (1979).

KCROFE $C_{12}H_{24}O_6 \cdot K^{+} \cdot (C_{44}H_{28}N_4Fe(SC_6H_5)_2^{-})$; M. P. Byrn and C. E. Strouse: *J. Am. Chem. Soc.* **103**, 2633 (1981).

KTHOXD $C_{12}H_{24}O_6 \cdot$ KNCS: P. Seiler, M. Dobler and J. D. Dunitz: *Acta Crystallogr.* **B30**, 2744 (1974).

NACNPA $C_{12}H_{24}O_6 \cdot Na^{+} \cdot PBr_2(CN)_2^{-} \cdot (C_4H_8O)$; W. S. Sheldrick, A. Schmidpeter, F. Zwaschka, K. B. Dillon, A. W. G. Platt and T. C. Waddington: *J. Chem. Soc., Dalton Trans.* 415 (1981).

NACNPB $C_{12}H_{24}O_6 \cdot Na^{+} \cdot PBr(CN)_3^{-} \cdot 2(C_4H_8O)$; W. S. Sheldrick, A. Schmidpeter, F. Zwaschka, K. B. Dillon, A. W. G. Platt and T. C. Waddington: *J. Chem. Soc., Dalton Trans.* 415 (1981).

NACRWA $C_{12}H_{24}O_6 \cdot Na^{+} \cdot (W(CO)_5SH^{-})$; M. K. Cooper, P. A. Duckworth, K. Hendrick and M. McPartlin: *J. Chem. Soc., Dalton Trans.* 2357 (1981).

NACRWB $C_{12}H_{24}O_6 \cdot Na^{+} \cdot (W_2(CO)_{10}SH^{-})$; M. K. Cooper, P. A. Duckworth, K. Hendrick and M. McPartlin: *J. Chem. Soc., Dalton Trans.* 2357 (1981).

NATHOD $C_{12}H_{24}O_6 \cdot$ NaNCS $\cdot H_2O$; M. Dobler, J. D. Dunitz and P. Seiler: *Acta Crystallogr.* **B30**, 2741 (1974).

RBTHXD $C_{12}H_{24}O_6 \cdot$ RbNCS; M. Dobler and R. P. Phizackerley: *Acta Crystallogr.* **B30**, 2746 (1974).

SUCCIN $C_{12}H_{24}O_6 \cdot C_4H_6O_4 \cdot H_2O$; L. Parenteau and F. Brisse: *Can. J. Chem.* **67**, 1293 (1989).

TETCS $C_{16}H_{23}O_{14}^{-} \cdot Cs^{+} \cdot 2H_2O$; P. J. Dutton, F. R. Fronczek, T. M. Fyles, R. D. Gandour and V. V. Suresh: submitted.

TETEN $C_{16}H_{24}O_{14} \cdot C_2N_2H_g \cdot 3H_2O$; J. J. Daly and P. Schönholzer: *Helv. Chim. Acta* **64**, 1444 (1981).

TETH $C_{16}H_{24}O_{14} \cdot 2H_2O$; P. J. Dutton, F. R. Fronczek, T. M. Fyles and R. D. Gandour: *J. Am. Chem. Soc.* **112,** 8984 (1990).

TETNA $C_{16}H_{23}O_{14}^{-} \cdot Na^{+} \cdot 2H_2O$; P. J. Dutton, F. R. Fronczek, T. M. Fyles, R. D. Gandour and V. V. Suresh: submitted.

TETTL $C_{16}H_{23}O_{14}^{-} \cdot Tl^{+} \cdot 2H_2O$; P. J. Dutton, F. R. Fronczek, T. M. Fyles, R. D. Gandour and V. V. Suresh: submitted.

XOCCPN $(C_{12}H_{24}O_6 \cdot Na^{+})_2 \cdot (P(CN)_2 \cdot 2(C_4H_8O)$; W. S. Sheldrick, J. Kroner, F. Zwaschka and A. Schmidpeter: *Angew. Chem. Int. Ed. Engl.* **18**, 934 (1979).